

Hemodynamic changes in four aneurysms leading to their rupture at follow-up periods

Hemodynamické změny ve čtyřech aneurysmatech vedoucí k jejich ruptuře v průběhu sledování

Abstract

Hemodynamic parameters play a significant role in the development of intracranial aneurysms and their time-depending changes during a prolonged follow-up period could lead to an increasing risk of rupture or to aneurysm rupture. The characteristics of these changes could bring significant information about the development of aneurysms and their rupture. In this unique study, we analyzed four incidental unruptured intracranial aneurysms in four patients who were followed-up for a mean period of 5 years until their rupture. We performed computational fluid dynamic simulations with the data from two or three follow-up angiographic examinations from each patient and analyzed the results with regard to time-dependent changes in terms of the values of hemodynamic parameters. Except one aneurysm of a fusiform dissecting origin, three aneurysms on MRA were described as non-growing. In the aneurysm domes, the minimal wall shear stress decreased and the low wall shear stress area increased significantly over time; the results indicated that the time-dependent changes such as decreasing values of minimal wall shear stress and increasing values of low wall shear stress area could lead to an increased risk of rupture. For accurate evaluation of the rupture risk using computational fluid dynamic simulation, it is important to analyze more than two models of aneurysm during a follow-up period and focus on significant changes in the values of hemodynamic parameters.

Souhrn

Hemodynamické parametry hrají významnou roli ve vývoji intrakraniálních aneurysmat a jejich změny v průběhu dlouhodobého sledování mohou vést ke zvýšení rizika ruptury či k samotné ruptuře aneurysmat. Definování těchto změn by významně přispělo k pochopení vývoje a ruptury aneurysmatu. V této jedinečné práci jsou analyzována data čtyř incidentálních neprasklých intrakraniálních aneurysmat u čtyřech pacientů, kteří byli sledováni v průměru po dobu 5 let až do chvíle ruptury aneurysmatu. Bylo provedeno matematické modelování hemodynamiky z dostupných dvou až tří angiografických vyšetření od každého pacienta, získaných během sledování, a změny hodnot hemodynamických parametrů byly analyzovány. Až na jedno, původně fusiformní, disekující aneurysma, velikost tří aneurysmat byla popsána na vyšetření MRA jako stacionární. Hodnoty minimálního smykového napětí se významně snížily a velikost oblasti s minimálním smykovým napětím ve vaku aneurysmat se významně zvýšily v průběhu času a výsledky naznačily podíl snižujících se hodnot smykového tření a rostoucí oblasti nízkého smykového napětí v průběhu času na zvyšování rizika ruptury aneurysmatu. K přesnému posouzení rizika ruptury aneurysmatu pomocí matematického modelování hemodynamiky, je nutné analyzovat více než dva modely aneurysmat a zaměřit se na signifikantní změny v hodnotách hemodynamických veličin.

The Editorial Board declares that the manuscript met the ICMJE "uniform requirements" for biomedical papers.

Redakční rada potvrzuje, že rukopis práce splnil ICMJE kritéria pro publikace zaslané do biomedicínských časopisů.

A. Sejkorová¹, H. Švihlová², O. Petr³, K. D. Dennis⁴, S. Uthamaraj⁴, G. Lanzino⁵, M. Sameš¹, D. Dragomir-Daescu⁶, A. Hejčl^{1,7,8}

¹ Department of Neurosurgery, J. E. Purkyně University, Masaryk Hospital, Ústí nad Labem, Czech Republic

² Mathematical Institute of Charles University, Prague, Czech Republic

³ Department of Neurosurgery, Medical University Innsbruck, Innsbruck, Austria

⁴ Division of Engineering, Mayo Clinic, Rochester, MN, USA

⁵ Department of Neurological Surgery, Mayo Clinic, Rochester, MN, USA

⁶ Department of Physiology and Biomedical Engineering, Mayo Clinic, Rochester, MN, USA

⁷ International Clinical Research Center, St. Anne's University Hospital, Brno, Czech Republic

⁸ Institute of Experimental Medicine, Academy of Sciences of the Czech Republic, Prague, Czech Republic



Alena Sejkorová, MD
Department of Neurosurgery
Masaryk Hospital
Sociální péče 3316/12A
400 11 Ústí nad Labem
Czech Republic
e-mail: alena.sejkorova@gmail.com

Accepted for review: 2. 4. 2020

Accepted for print: 5. 11. 2020

Key words

aneurysm – computational fluid dynamic – low wall shear stress area – wall shear stress

Klíčová slova

aneurysma – matematické modelování hemodynamiky – oblast nízkého smykového napětí – smykové napětí

Introduction

In the past few years, we observed a rapidly growing area of research which computationally analyzes blood hemodynamic in the intracranial vessels and aneurysms. Usually, the clinicians could rely on some clinical and morphological parameters which could help predict the risk of aneurysm rupture. However, it is understood that the blood flow and hemodynamic parameters play an important role in the development of intracranial aneurysms [1–3]. Parameters such as pressure, velocity, or wall shear stress (WSS) on the endothelial cell of the vessels change in time and these changes contribute to modification of the histological characteristic of the wall, which could lead to an increased risk of aneurysm rupture [4–6]. The information on these changes in time could help specify concrete hemodynamic parameters and their time changes which best define an increased risk of aneurysm rupture.

To date, no study analyzing two or more data sets (before rupture) of patients with eventually ruptured incidental aneurysm in the follow-up period has been published. Skodvin et al analyzed one angiographic examination of unruptured aneurysms prior to their rupture [7] with a finding that the

hemodynamic parameters in later ruptured aneurysms evolve during a follow-up period and that the increased low wall shear stress area (LSA) might predict a rupture of aneurysm. The number of patients with ruptured incidental aneurysms at follow-up is really low, but these patients could provide the most accurate information about the development of aneurysms ruptured in the future [8]. The data obtained in this way could facilitate the decision about the therapy of incidental unruptured aneurysm and could help decide whether it is safe to choose conservative therapy over intervention.

To make progress in this direction, we collected records of all patients with unruptured intracranial aneurysms who were followed-up at an outpatient clinic between 2000 and 2016. These records were retrospectively reviewed in two large tertiary referral centers. In our study, we included four patients who met the criteria of having two or more high-quality angiography imaging investigations performed before aneurysm rupture. Computational fluid dynamic (CFD) simulations were performed using the angiography images to analyze the hemodynamic changes in aneurysms at follow-up and to find which hemodynamic parameters

correlated with an increased risk of rupture or with the rupture itself.

Materials and methods

Patients and aneurysms

Two patients' databases from Masaryk Hospital, Ústí nad Labem, Czech Republic, and from Mayo Clinic, Rochester, MN, USA, were available for the analysis. A total of four patients with one unruptured intracranial aneurysm each were followed-up at an outpatient clinic for a mean period of 5 years and 3 months (from 4 years and 7 months to 8 years and 7 months). Two aneurysms were localized in the anterior circulation, on the posterior communicating artery and on the anterior communicating artery, and two in the posterior circulation, on the posterior cerebral artery and on the basilar artery. In these years, they were referred more than once to the Radiology Department to obtain control images of unruptured intracranial aneurysm by MRA or CTA and visited the Outpatient Clinic for Neurosurgery, where the results of CTA or MRA were interpreted to the patient and the decision of conservative treatment was made. The patients' radiological records were analyzed to find high quality angiographic examinations and

Tab. 1. Characteristic of patients and aneurysms.

Variables of patients		Patient 1			Patient 2		Patient 3			Patient 4	
gender		woman			woman		woman			woman	
year of birth		1959			1925		1930			1944	
period from the first to last examination		12/1998–06/2007			01/2005–06/2010		08/2007–02/2011			08/2003–08/2008	
comorbidities		morbid obesity, psychiatric diagnosis, transient ischemic attack			none		diabetes mellitus, arterial hypertension, hyperlipidemia, chronic renal failure			carotid artery stenosis	
outcome		death after one month			GOS 5		death			death	
aneurysm localization		posterior cerebral artery			posterior communicating artery		basilar artery			anterior communicating artery	
Variables of aneurysms	year of examination angiographic method	1998	2006	2007	2005	2010	2007	2008	2011	2003	2008
		MRA	MRA	MRA	CTA	MRA	MRA	MRA	MRA	MRA	MRA
		fusiform dilatation	8.8	15.5	10.2	12.3	4.8	5.5	6.0	2.4	2.3
			8.7	10.5	8.9	9.4	5.3	4.8	5.3	1.7	1.7
			1.0	2.3	1.2	1.4	0.9	1.1	1.2	1.5	1.6

GOS – Glasgow Outcome Score

Tab. 2. Hemodynamic parameters – systolic peak values.

Variables	year of examination	Patient 1			Patient 2		Patient 3			Patient 4	
		1998	2006	2007	2005	2010	2007	2008	2011	2003	2008
mean WSS (Pa)		5.99	0.69	0.17	0.15	0.12	6.86	6.63	7.22	3.66	3.78
max WSS (Pa)		18.92	5.34	1.64	0.81	0.76	15.13	17.58	19.30	54.66	47.27
min WSS (mPa)		57.00	17.60	0.30	12.80	1.41	117.60	97.70	77.90	221.70	31.40
normalized WSS		0.74	0.13	0.04	0.20	0.20	1.59	1.21	1.36	0.58	0.52
LSA (%)		9.22	65.74	87.58	38.87	50.81	0.20	0.65	0.94	10.05	38.64
mean velocity (m/s)		0.22	0.05	0.02	0.03	0.02	0.23	0.22	0.23	0.10	0.10
max velocity (m/s)		0.73	0.45	0.23	0.15	0.15	0.77	0.83	0.79	0.58	0.61

LSA – low wall shear stress area proportion; WSS – wall shear stress

a total of ten examinations were selected for the process of segmentation (Tab. 1).

Imaging data and hemodynamics modeling

Nine and one DICOM file sets were obtained from diagnostic MRA and CTA examinations, respectively; these two noninvasive modalities are standard instruments for follow-up control images. The reconstructed images from CTA contained 512×512 pixels with a pixel spacing of 0.48 mm and slice thickness of 1 mm. In the MRA images from 1.5 Tesla machine, the slices were of 512×512 pixels with spacing of 0.7 mm between the slices. The segmentations using DICOM file sets were done by one neurosurgeon using the software Mimics 16.0 (Materialise, Leuven, Belgium) and, afterwards, the segmentation was evaluated by another neurosurgeon. The geometry was obtained using the thresholding of vessels algorithm and the region growing algorithm. The artery inlet was kept as long as possible in the anterior circulation with a minimum of two turns and the posterior circulation with the length of basilar artery and was cut at the same locations in all the models of the same aneurysm [9]. The vascular 3D model was smoothed in 3-matic 8.0 (Materialise, Leuven, Belgium). To perform CFD simulations, a tetrahedral grid was used with a maximum element size of 0.15 mm and with 7 inflation layers in the boundary layer (the thickness of the first layer at the vessel surface was fixed at 0.01 mm and the inflation factor ratio was 1.35). The grid was constructed using ICEM CFD (ANSYS, Canonsburg, IA, USA). A grid sensitivity study was conducted to ensure that the results were grid-independent [10]. The CFD simulations were performed as de-

scribed by Hodis et al [10]. Briefly, using the software ANSYS Fluent 16.1 (ANSYS, Canonsburg, PA, USA), the blood flow simulation was performed considering the blood an incompressible Newtonian fluid, with the density of 1050 kg/m^3 , dynamic viscosity of 3.7 cP and kinematic viscosity of $3.5 \times 10^{-6} \text{ m}^2/\text{s}$; the vessel walls were assumed rigid and the blood flow was considered laminar. At the extended circular inlets surface, the flow was prescribed by a pulsatile Womersley velocity profile with a transient waveform given by Zamir and used by Hodis and Zamir [11–13]. For traction-free conditions at the outlets, we extended the outlet branches to the same length in a concrete model and the zero-velocity boundary conditions were set. The simulations were conducted for four cardiac cycles to ensure that there were no numerical transients in the solution. The result from the fourth cardiac cycle served as a source for hemodynamic parameters computations.

Data Analysis

Patients' information including the follow-up period, gender, comorbidities and outcome were recorded (Tab. 1). We also recorded the localization of the aneurysms, their maximal diameter (largest perpendicular distance between the neck plane and the aneurysm dome), the maximal neck diameter and the aspect ratio (the ratio of the maximum perpendicular height to the average neck diameter) (Tab. 1). The hemodynamic parameters are shown in Tab. 2; they include WSS, normalized WSS defined as a ratio of mean WSS distributions to the average parent vessel WSS, minimal and maximal WSS, oscillatory shear index (OSI), velocity and LSA; the areas of the aneurysm wall

exposed to a WSS value below 10% of the mean parent vessel WSS value were defined as previously described and visualized using the Tecplot 360 (Tecplot Inc., Bellevue, WA, USA) software [14–16]. The aneurysm domes were separated using Tecplot 360 function of creating a plane from a manually created line made from the points in the aneurysm neck's line.

Results

All patients were women, the mean age at the time of the first examination was 64 years. The follow-up period was 5.6 years in average, for details, see Tab. 1. Three patients had metabolic syndrome with complications and died after the rupture of the aneurysms. The last one, Patient 2, was in a good condition without comorbidities and her outcome was evaluated as Glasgow Outcome Score 5.

The size development of the aneurysms defined by three parameters – maximal diameter, neck diameter and aspect ratio – is shown in Tab. 1. Only the posterior cerebral artery aneurysm in Patient 1 was significantly growing with thrombotic development; in the first examination, the aneurysm was fusiform and in the next 9 years, it grew up to a maximum diameter of 15.5 mm. In other three patients, the aneurysms in MRA images were described as non-growing; however, we can see small differences in their size after parameter measurement in 3D models (Tab. 1). The aneurysm in Patient 2 developed two blebs.

Table 2 shows the values of the hemodynamic parameters at peak systole. The changes in minimal WSS and LSA values at follow-up (from the first to the last examination before rupture) were greater than the changes in other hemodynamic parameters.

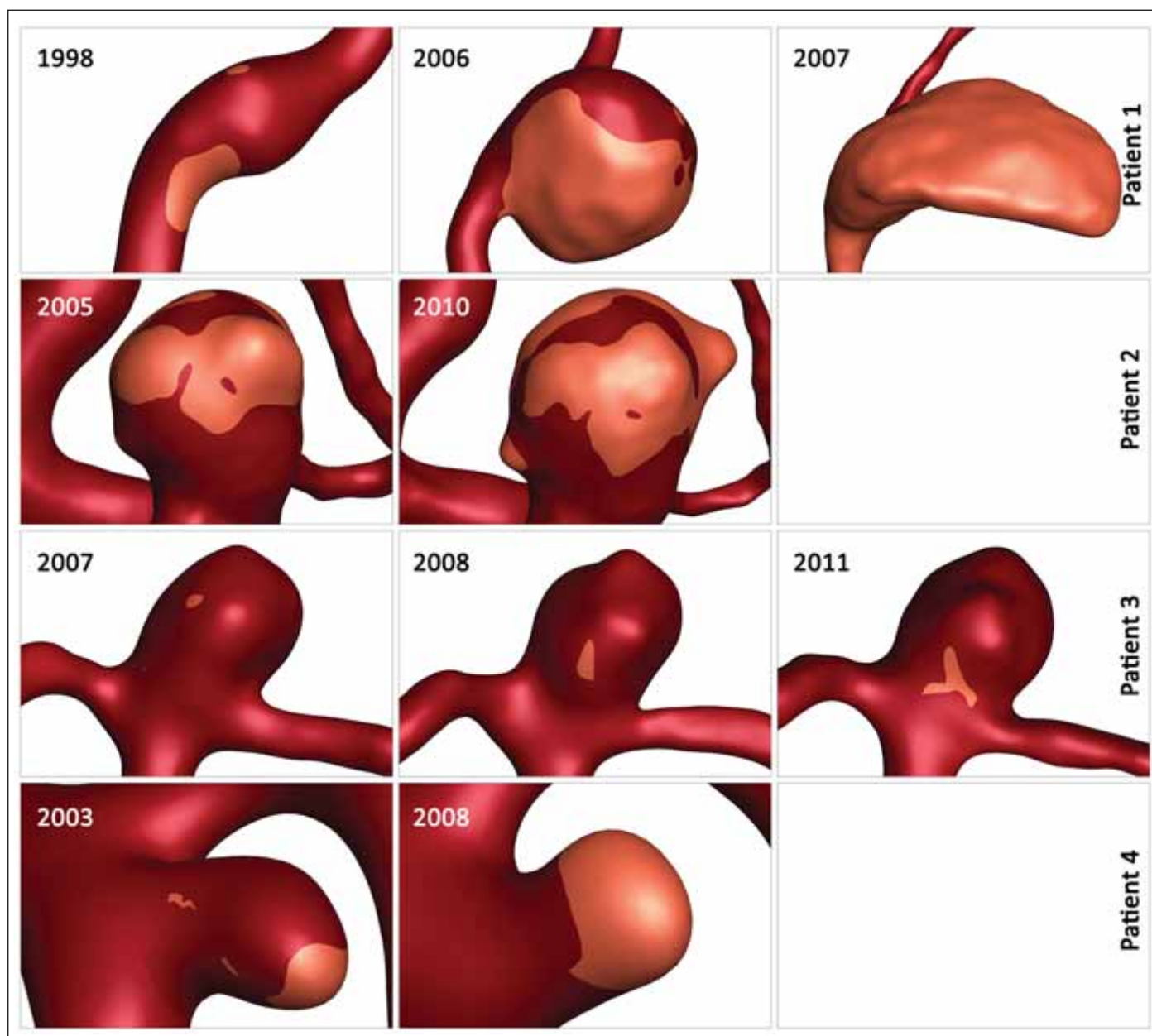


Fig. 1. Images of proportional layout of low wall shear stress area. Overview of the space enlargement of the low wall shear stress area in four aneurysm during their follow-up period.

Obr. 1. Proporční rozložení oblasti s nízkým smykovým napětím. Přehled zvětšování oblasti s nízkým smykovým napětím ve čtyřech aneurysmatech během sledování.

ters (Tab. 2). The minimum WSS and LSA decreased by one and two orders of magnitude, respectively. In Patient 1, the decrease of minimal WSS values between the second and the third examination was 33.2%, in Patient 2, the difference was 89%, in Patient 3, the minimal WSS decreased by 33.8% and in Patient 4, the minimal WSS at the last examination was by 85.8% smaller than at the first examination. The LSA in Patients 1, 2, 3 and 4 increased by 849.9, 30, 370 and 284.5%, respectively. The proportional layout of LSA is shown in Fig. 1.

Discussion

We hypothesized that the time-dependent changes in hemodynamic parameters in intracerebral aneurysms led to an increased risk of rupture. Our study analyzed the hemodynamic simulation results in the unruptured aneurysms from four patients at two or three different time points before rupture, which make this study unique. The results indicate that the time-dependent changes such as decreasing values of minimal WSS and increasing values of LSA could indicate an increased risk of rupture.

Many publications compare the characteristics in ruptured vs. unruptured aneurysms in order to define the hemodynamic factors associated with rupture [17–19]. However, such studies do not take into consideration that after the rupture of the aneurysm, its morphology and, subsequently, values of hemodynamic parameters could change [7,20]. Thus, we are assuming that the calculated values after the aneurysm rupture which increased the rupture risk and led to the aneurysm rupture could be misleading because of the change in the geom-

etry as well as in the hemodynamic and flow patterns.

Possibly, not the values themselves but the time-dependent changes of the values might be more important in therapy decision-making. The fitting examples are the values of the hemodynamic parameters of intracranial aneurysms in the anterior or posterior circulation [21]. There are studies declaring that the low WSS is the main factor leading to the grow or rupture of aneurysms, and vice versa [22–26]. Both theories have the basic explanation in histologic analyses of the aneurysm wall and they both could play a role in the time-dependent changes in intracranial aneurysm blood flow and subsequent rupture risk [27]. However, the exact values leading to rupture are difficult to find.

Therefore, it is very important to analyze time-dependent changes of the hemodynamic parameters in the same aneurysm before rupture. Patients with aneurysms ruptured in follow-up periods are extremely rare [8,28]. Mostly, the patients are older, and the aneurysms are small; however, in our cases, the aneurysms differ in size, from 2 to 15 mm. Skodvin et al or Takao et al analyzed unruptured aneurysms before their rupture and matched the studied aneurysms with control unruptured aneurysms, but they performed only one examination before the rupture and therefore, they could not provide any information about the time-dependent changes of the hemodynamic parameters [7,29]. One set of results where we do not know the exact values of the hemodynamic parameters which could lead to the rupture is likely to be not sufficient. In the clinical practice, the neurosurgeons will need the information about the ongoing changes which would take place in the aneurysm, they probably need CFD simulations of at least two subsequent angiographic examinations.

In our study, the changing parameters that seem to correlate with an increased rupture risk include the minimal WSS and LSA. Skodvin et al reached a similar conclusion [7]. The most noticeable progress is seen in LSA, where the LSA increase in Patients 1, 3 and 4 exceeds 200%. However, we need to take in consideration the morphologic development of the aneurysm in Patient 1, where the aneurysm size increased from a fusiform shape to 15.5 mm and the aneurysm was partially thrombosed, and in Patient 2, where 2 blebs originated from the

aneurysm dome. In models with visualized values of LSA, it is possible to notice the shift of the area to the bleb area in Patient 2 and the influence of low WSS on the part of the aneurysm dome in Patient 2 where a thrombotic process took place (Fig. 1).

Limitation

As previously mentioned, the CFD studies still have many limitations delaying their use in the clinical practice [30,31]. Specifically, we did not have the patient flow profile data, and we used the flow that was described by a pulsatile Womersley velocity profile with a transient waveform. This simplification might contribute to the computed flow pattern results. Further contributing factors are the simplification of the vessel wall characteristics, physical properties of the blood, and the outflow boundary conditions.

This study only analyzes the data from four patients with aneurysms at different location, making it difficult to draw general conclusions and recommendations.

Conclusion

The hemodynamic changes during a prolonged time do not fully explain the complex process of aneurysm growth and rupture. Therefore, CFD simulations in the future could only serve as an additional supporting examination that could help the neurosurgeon in the decision-making process. However, these unique results describing the time-dependent changes in the hemodynamic parameters in intracranial aneurysms during a prolonged time could encourage the clinician to explore the possibility of CFD simulation results to correlate with a rupture risk. Obtaining more data about the possible future behavior of unruptured intracranial aneurysms which are feasible to get analyze in a few days or weeks, could decrease the risk that the patient is taking on the advice of their clinician. Generally, the growth of unruptured aneurysms is periodically checked by angiographic tests. Analyzing these data via CFD simulations, we obtain the values of hemodynamics parameters in a follow-up period and, comparing them, we can gain more information about the character of the aneurysm. As in many other situations in the clinical practice, the values of parameters changing in time considerably indicate possible pathological development, such as the decrease of WSS or the increase of LSA in the case of intracranial aneurysms.

Ethical principles

This retrospective study has been approved by the Mayo Clinic IRB 15-001870 and has been performed in accordance with the ethical standards.

Financial support

Supported by project No. LQ1605 from the National Program of Sustainability II (MEYS CR), by International Clinical Research Center of St. Anne's University Hospital Brno project No. CZ.1.05/1.1.00/02.0123 (OP VaVpl), with a grant No. 17-32872A from the Czech Health Research Council (AZV ČR), grants No. IGA- KZCR-2018-2-7, IGA- KZCR-2018-2-8, IGA- KZCR-2018-2-9 by the Internal Grant Agency of the Krajská zdravotní.

Conflict of interest

The authors declare they have no potential conflicts of interest concerning the drugs, products or services used in the study.

References

1. Cebral JR, Mut F, Weir J et al. Association of hemodynamic characteristics and cerebral aneurysm rupture. *AJNR Am J Neuroradiol* 2011; 32(2): 264–270. doi: 10.3174/ajnr.A2274.
2. Qiu T, Jin G, Xing H et al. Association between hemodynamics, morphology, and rupture risk of intracranial aneurysms: a computational fluid modeling study. *Neurrol Sci* 2017; 38(6): 1009–1018. doi: 10.1007/s10072-017-2904-y.
3. Soldozy S, Norat P, Elsarraig M et al. The biophysical role of hemodynamics in the pathogenesis of cerebral aneurysm formation and rupture. *Neurosurg Focus* 2019; 47(1): E11. doi: 10.3171/2019.4.focus19232.
4. Frösen J, Piippo A, Paetau A et al. Remodeling of sacular cerebral artery aneurysm wall is associated with rupture. *Stroke* 2004; 35(10): 2287–2293. doi: 10.1161/01.STR.0000140636.30204.da.
5. Cebral JR, Detmer F, Chung BJ et al. Local hemodynamic conditions associated with focal changes in the intracranial aneurysm wall. *AJNR Am J Neuroradiol* 2019; 40(3): 510–516. doi: 10.3174/ajnr.A5970.
6. Staarmann B, Smith M, Prestigiacomo CJ. Shear stress and aneurysms: a review. *Neurosurg Focus* 2019; 47(1): E2. doi: 10.3171/2019.4.focus19225.
7. Skodvin TO, Evju O, Helland CA et al. Rupture prediction of intracranial aneurysms: a nationwide matched case-control study of hemodynamics at the time of diagnosis. *J Neurosurg* 2017; 129(4): 854–860. doi: 10.3171/2017.5.JNS17195.
8. Juvela S, Porras M, Heiskanen O. Natural history of unruptured intracranial aneurysms: a long-term follow-up study. *J Neurosurg* 1993; 79(2): 174–182. doi: 10.3171/jns.1993.79.2.0174.
9. Hodis S, Kargar S, Kallmes DF et al. Artery length sensitivity in patient-specific cerebral aneurysm simulations. *AJNR Am J Neuroradiol* 2015; 36(4): 737–743. doi: 10.3174/ajnr.A4179.
10. Hodis S, Uthamaraj S, Smith AL et al. Grid convergence errors in hemodynamic solution of patient-specific cerebral aneurysms. *J Biomech* 2012; 45(16): 2907–2913. doi: 10.1016/j.jbiomech.2012.07.030.
11. Womersley JR. Method for the calculation of velocity, rate of flow and viscous drag in arteries when the pressure gradient is known. *J Physiol* 1955; 127(3): 553–563. doi: 10.1113/jphysiol.1955.sp005276.
12. Hodis S, Zamir M. Pulse wave velocity as a diagnostic Index: the pitfalls of tethering versus stiffening of the arterial wall. *J Biomech* 2011; 44(7): 1367–1373. doi: 10.1016/j.jbiomech.2010.12.029.
13. Hodis S, Zamir M. Mechanical events within the arterial wall under the forces of pulsatile flow: a review.

J Mech Behav Biomed Mater 2011; 4(8): 1595–1602. doi: 10.1016/j.jmbbm.2011.01.005.

14. Xiang J, Natarajan SK, Tremmel M et al. Hemodynamic-morphologic discriminants for intracranial aneurysm rupture. Stroke 2011; 42(1): 144–152. doi: 10.1161/STROKEAHA.110.592923.

15. Mut F, Lohner R, Chien AC et al. Computational hemodynamics framework for the analysis of cerebral aneurysms. Int J Numer Method Biomed Eng 2011; 27(6): 822–839. doi: 10.1002/cnm.1424.

16. Cebral JR, Castro MA, Burgess JE et al. Characterization of cerebral aneurysms for assessing risk of rupture by using patient-specific computational hemodynamics models. AJNR Am J Neuroradiol 2005; 26(10): 2550–2559.

17. Cebral JR, Mut F, Weir J et al. Quantitative characterization of the hemodynamic environment in ruptured and unruptured brain aneurysms. AJNR Am J Neuroradiol 2011; 32(1): 145–151. doi: 10.3174/ajnr.A2419.

18. Liu J, Xiang J, Zhang Y et al. Morphologic and hemodynamic analysis of paraclinoid aneurysms: ruptured versus unruptured. J NeuroIntervent Surg 2014; 6(9): 658–663. doi: 10.1136/neurintsurg-2013-010946.

19. Berg P, Beuing O. Multiple intracranial aneurysms: a direct hemodynamic comparison between ruptured and unruptured vessel malformations. Int J Comput As-

sist Radiol Surg 2017; 13(1): 83–93. doi: 10.1007/s11548-017-1643-0.

20. Chien A, Sayre J. Morphologic and hemodynamic risk factors in ruptured aneurysms imaged before and after rupture. AJNR Am J Neuroradiol 2014; 35(11): 2130–2135. doi: 10.3174/ajnr.A4016.

21. Chien A, Castro MA, Tateishi S et al. Quantitative hemodynamic analysis of brain aneurysms at different locations. AJNR Am J Neuroradiol 2009; 30(8): 1507–1512. doi: 10.3174/ajnr.A1600.

22. Boussel L, Rayz V, McCulloch C et al. Aneurysm growth occurs at region of low wall shear stress. Stroke 2008; 39(11): 2997–3002. doi: 10.1161/STROKEAHA.108.521617.

23. Dolan JM, Kolega J, Meng H. High wall shear stress and spatial gradients in vascular pathology: a review. Ann Biomed Eng 2013; 41(7): 1411–1427. doi: 10.1007/s10439-012-0695-0.

24. Kadasi LM, Dent WC, Malek AM. Colocalization of thin-walled dome regions with low hemodynamic wall shear stress in unruptured cerebral aneurysms. J Neurosurg 2013; 119(1): 172–179. doi: 10.3171/2013.2.JNS.12968.

25. Zhou G, Zhu Y, Yin Y et al. Association of wall shear stress with intracranial aneurysm rupture: systematic review and meta-analysis. Sci Rep 2017; 7(1): 5331–5331. doi: 10.1038/s41598-017-05886-w.

26. Shojima M, Oshima M, Takagi K et al. Magnitude and role of wall shear stress on cerebral aneurysm. Stroke 2004; 35(11): 2500–2505. doi: 10.1161/01.STR.0000144648.89172.0f.

27. Meng H, Tutino VM, Xiang J et al. High wss or low wss? Complex interactions of hemodynamics with intracranial aneurysm initiation, growth, and rupture: toward a unifying hypothesis. AJNR Am J Neuroradiol 2014; 35(7): 1254–1262. doi: 10.3174/ajnr.A3558.

28. Investigators TU. The natural course of unruptured cerebral aneurysms in a Japanese cohort. N Engl J Med 2012; 366(26): 2474–2482. doi: 10.1056/NEJMoa1113260.

29. Takao H, Murayama Y, Ishibashi T et al. CFD reveals hemodynamic differences between unruptured and ruptured intracranial aneurysms during observation. Stroke 2012; 43: A2731. doi: 10.1161/str.43.suppl1.A2731.

30. Berg P, Saalfeld S, Voß S et al. A review on the reliability of hemodynamic modeling in intracranial aneurysms: why computational fluid dynamics alone cannot solve the equation. Neurosurg Focus 2019; 47(1): E15. doi: 10.3171/2019.4.focus19181.

31. Steinman DA, Pereira VM. How patient specific are patient-specific computational models of cerebral aneurysms? An overview of sources of error and variability. Neurosurg Focus 2019; 47(1): E14. doi: 10.3171/2019.4.focus1912.

Poděkování partnerům České neurologické společnosti



platinoví partneři



zlatí partneři



bronzový partner



*Partner vzdělávacího portálu
www.CzechNeurOnline.cz*